Nrf2 Regulates Microglia-mediated Phagocytosis and Neuroinflammation After Intracerebral Hemorrhage

Lirong Liu
Shanxi Medical University
Shuangjin Bao
Shanxi Medical University https://orcid.org/0000-0002-0450-0307
Zhenjia Yao
Shanxi Medical University
Qinqin Bai
Shanxi Medical University
Chuntian Liang
Shanxi Medical University
Pengcheng Fu
Shenzhen Longhua New District People's Hospital
Gaiqing Wang (wanggq08@163.com)
Shanxi Medical University https://orcid.org/0000-0002-8977-1383

Research Article

Keywords: Microglia, Phagocytosis, Neuroinflammation, Intracerebral hemorrhage, Trem1, Trem2

Posted Date: February 25th, 2022

DOI: https://doi.org/10.21203/rs.3.rs-1373100/v1

Abstract

Background: Activated microglia is essential for hematoma clearance and recovery after intracerebral hemorrhage (ICH). This study aims to evaluate the effect of microglial functional transformation in hematoma clearance after ICH. Through *in vitro* and *in vivo* experiments, we also investigate whether Nuclear factor erythroid 2-related factor 2 (*Nrf2*) -mediated microglial phagocytosis and inflammatory response plays a role in hematoma clearance and functional recovery after ICH.

Methods: For *in vitro* experiments, BV-2 cells were cultured and randomly divided into 4 groups, including normal control, microglia + *Nrf2*-siRNA (100 nmol/L), microglia + monascin (15 μM), and microglia + Xuezhikang (200 μg/mL) groups. For *vivo* experiments, 42 mice were divided into2 groups, i.e., sham, ICH+vehicle, ICH+*Nrf2*-/-, ICH+monascin (10mg/kg/day, twice) and ICH+Xuezhikang (0.2g/kg/day, twice) groups. Further, neurologic scores, hemoglobin levels, microglial phagocytosis, brain expression of *CD80*/ *Trem1*/ *TNF*-α (pro-inflammatory cytokines),and *CD206*/ *Trem2*/ *BDNF*(anti-inflammatory cytokines) were analyzed 72 hours after surgery.

Results: The results showed that *Nrf2* agonists improved neurological deficits and decreased hemoglobin levels after ICH through regulating microglial functional transformation. Administration of *Nrf2* agonist-monascin/ Xuezhikang improved microglia-mediated phagocytosis of erythrocytes and bio-particles through *Nrf2* upregulation. Alternatively, monascin/ Xuezhikang promoted the expression of Triggering receptor II expressed on myeloid cells(*Trem2*), *CD206,* and *BDNF* while inhibiting the expression of *Trem1*,*CD80,* and *TNF*-α in microglia. Conversely, *Nrf2* inhibition (*Nrf2* siRNA or *Nrf2*-/-) demonstrated conflicting results after ICH.

Conclusion: Microglial functional transformations are implicated in hematoma clearance after ICH. *Nrf2* activation leads to microglial functional transformation and phagocytic responses then exert its neuroprotection after ICH. *Nrf2* activator (Monascin /Xuezhikang) improves hematoma clearance and alleviates neuroinflammation by regulating microglial functional alteration after ICH.

1 Introduction

Intracerebral hemorrhage (ICH) is a devastating stroke subtype, with high morbidity and mortality [1–3]. Accumulating evidence suggests that hematoma and its degradation products primarily cause a poor prognosis after ICH[4]. Recent studies show that microglia and endogenous scavenging system [5], (a novel effective therapeutic approach for ICH) regulate the process of hematoma clearance[4, 6].

Microglia are activated by diverse pathologic events or changes in brain homeostasis. Activated microglia are divided into pro-inflammatory and anti-inflammatory functional states after ICH[7, 8]. Pro-inflammatory phenotype is characterized by the production of tumor necrosis factor-α (*TNFα*), interleukin *1β* (*IL-1β*), *CD80*, *CD86*, and *CD16/32*, etc.; it induces neuron cell death and promotes neuroinflammation. On the other hand, anti-inflammatory phenotype attenuates inflammation, manipulates phagocytosis,

and promotes neural repair in the presence of *IL-4*, *IL-10*, brain-derived neurotrophic factor (*BDNF*), and *CD206*,etc.[9–11].Triggering receptor I expressed on myeloid cells (*Trem1*) is a crucial inflammatory amplifier of microglia [12, 13]. On the other hand, triggering receptor II expressed on myeloid cells (*Trem2*) exerts anti-inflammatory and neuroprotective effects. It might be a receptor that regulates phagocytosis [14, 15].

Nuclear factor erythroid 2-related factor 2 (*Nrf2*) and peroxisome proliferator-activated receptor *γ* (*PPARγ*) has attracted significant research attention due to its role in the clearance of endogenous hematomas as regulators [16, 17]. Besides, they potentially promote the removal of erythrocytes and hematoma remnants by interacting with *Trem1* or *Trem2*.

In our previous work, we confirmed that *Nrf2* agonist-monascin facilitates hematoma clearance and exerts neuroprotection after ICH[18, 19].Nonetheless, studies on the underlying mechanism of hematoma clearance and its neuroprotection of *Nrf2* have not reached maturity.

Therefore, this research further evaluated the natural *Nrf2* expression as well as its relationship with *Trem2* and *Trem1* after ICH. Then, we explored the mechanism and effects of *Nrf2* on phagocytic activity and the transformation of microglia-mediated neuroinflammation using *Nrf2* agonists monascin /Xuezhikang. Notably, monascin here acts as a novel type of *Nrf2* agonist and an agonist of peroxidase proliferator-activated receptor gamma (*PPAR-*); whereas Xuezhikang is an extract of cholestin that harbors monascin as its primary component. We also used *Nrf2*-siRNA via *in vitro* experiments or *Nrf2*-/- via *in vivo* experiments to provide strong evidence supporting the *Nrf2* as an effective treatment approach for ICH.

2 Materials And Methods

2a. Materials and methods

In our previous study, we showed that *TREM-1* inhibition improves neurological deficits and brain edema in subarachnoid hemorrhage [20].

2.1a. Cellular materials

Experimental cells: BV-2 cells (Solebo)

2.2a. Cellular experimental methods

2.2.1. Experimental cell groups

Normal group, siRNA group, monascin group, Xuezhikang group

2.2.2. Cell culture

BV-2 cells were cultured in a humidified incubator with 5% CO_2 at 37 °C. After 2-3 days, Dulbecco's Modified Eagle Medium (DMEM) was replaced, and non-adherent cells were removed. When the primary cultures reached 80% confluence, cells were harvested using 0.25% trypsin–EDTA solution and sub-cultured. Thereafter, the third passage of cells was selected for subsequent experiments.

2.2.3. Screening of Monascin/Xuezhikang concentration and the transfection sequence of Nrf2-siRNA by qPCR

RT-PCR was used to detect the *Nrf2*-mRNA levels, screen its best sequence, and the best drug concentrations of monascin or Xuezhikang. Exactly 1 ml aliquots of 5, 15, 30 μmol/L monascin or 100, 200, 500ug/ml Xuezhikang was added to a 12-well plate with three multiple holes in each group, and *Nrf2* interference vector(*siNrf2*) were synthesized (GenePharma, Shanghai, China), then transfected by incubating in DMEM containing GP-transfect-Mate (GenePharma, Shanghai, China).

Total RNA was extracted using the Trizol reagent. First-strand cDNA was synthesized using the PrimeScript RT Master Mix Kit (ABI-Invitrogen, Thermo Fisher Scientific, Grand Island, NY, USA), while β-Actin was used as the internal control. The quantification of endogenous control mRNA levels was performed using TaqMan assays. The data were analyzed using the $2^{-\triangle\triangle Ct}$ method.

The *Nrf2*-siRNA (100 nM) primer sequences screened by RT-PCR exhibited sense chain GCAGGACAUGGAUUUGAUUTT and antisense chain AAUCAAAUCCAUGUCCUGCTG. Then, 15μmol/L monascin or 200ug/ml Xuezhikang were selected for subsequent experiments.

2.2.4. Cell immunofluorescence

The immunofluorescence was performed as previo usly described[21]. The BV2 microglial cells were treated using *Nrf2*-siRNA, monascin, and Xuezhikang, respectively. The cells were collected and fixed with 4% paraformaldehyde, permeabilized using 0.5% Triton X-100, then blocked with goat serum for 60 min. The samples were overnight incubated with primary antibodies (anti-*Nrf2*, anti-*Trem1*, anti-*Trem2*, anti-*CD80*, anti-*CD206*, Abcam) at 4 ℃, incubated with a fluorescent dye-conjugated secondary antibody in the dark for 1 h, then stained using 4',6-diamidino-2-phenylindole (DAPI). Three different visual fields were randomly selected for each sample and photographed under a fluorescence microscope (LeicaDmil, Germany).

2.2.5. Phenotype of BV-2 cells detected by flow cytometry

The BV-2 cells were inoculated and 100 µL cell suspension with a final concentration of 10×10^6 cells/mL was pipetted into a round-bottom Eppendorf tube. After incubation with the primary antibody *CD80*/ *CD206* (anti-*CD80* 1:50, anti-*CD206* 1:50 Abcam) for 2h, the microglial cells were washed then incubated using a fluorescent-labeled secondary antibody for 1h. The total percentage of *CD206* and the relative ratio of *CD206* to *CD80* were determined through flow cytometry. Notably, *CD206* was shown as APC in the Q1 quadrant; *CD80* was displayed as fluorescein isothiocyanate (FITC) in the Q4 quadrant. The common mark was in the Q2 quadrant. The percentage of *CD206* and *CD80* (%) = $100 \times (Q1+Q2)/(Q2+Q4)$ was the phenotype of the microglia. The phenotype of the cells was evaluated by quantitative percentage.

2.2.6. Detection of Nrf2, Trem1, Trem2, CD80, CD206, TNF-α, and BDNF protein expressions via Western Blot (WB)

The BV2 cells were collected and treated with radioimmunoprecipitation (RIPA) lysis buffer and measured using a bicinchoninic acid (BCA) kit as previously described[8]. Equal amounts of protein were loaded on an SDS polyacrylamide gel, electrophoresed, then transferred to polyvinylidene fluoride (PVDF) membranes, which were then overnight incubated with primary antibodies (anti-*Nrf2*, anti-*Trem1*, anti-*Trem2*, anti-*CD80*, anti-*CD206*, anti-*TNF-α*, and anti-*BDNF*, Abcam) at 4 °C. The membranes were incubated with a horseradish peroxidase-conjugated secondary antibody and visualized through chemiluminescence. Densitometry was performed to quantify the signal intensity using ImageJ software (https://imagej.net).

2.2.7.1. Observation of phagocytosis of fluorescent bioparticles by immunofluorescence

The BV2 cells were treated with 10 mg/mL zymosan fluorescent bioparticles (Alexa Fluor594 conjugate; zymosan: BV-2 = 40:1) for 1 h,then fixed with 4% paraformaldehyde, before being permeabilized with Triton X-100. Then, the samples were placed in 10% goat serum for 2 h, overnight incubated with anti-*Iba1* antibody (1:100; Abcam) at 4 °C, then incubated with a FITC-conjugated secondary antibody. The phagocytosed bioparticles were observed using a fluorescence microscope.

2.2.7.2. Observation of phagocytosis of erythrocytes

After separation and purification of erythrocytes, they were counted and co-cultured with microglia at a ratio of 1:40 (microglia: erythrocytes). Microglia swallowing erythrocytes were observed using a microscope (Olympus CK40–32PH, Japan).

2b. Materials and methods

In our previous study, we found that *Nrf2* agonist -monascin facilitates hematoma clearance, alleviates cerebral edema, and exerts neuroprotection after ICH[18,19].

2.1b. Animal materials

Experimental male *Nrf2*-/-C57BL/6 mice (4–5 weeks old) were purchased from Cyagen Model Biological Research Center (Taicang) Co.,Ltd. (Suzhou, China), the other male C57BL/6 mice (4–5 weeks old) were purchased from the Animal Experimental Center of Shanxi Medical University. All animal experiments were approved and conducted as per the guidelines of the Ethics Committee of Shanxi Medical University, Shanxi, China. All surgical procedures were performed under anesthesia, and every effort was expended to minimize suffering.

2.2b. Animal experimental methods

2.2.1. Experimental design

A total of 42 mice were randomized to the following groups: sham (n = 8), ICH+ vehicle (n = 9), Nrf2-/-+ICH(n = 8), ICH+ monascin(10mg/kg/day, twice, n = 8), ICH+ Xuezhikang (0.2g/kg/day, twice, n = 9). Dead animals were replaced before final assessment. All gavages were administered by gastric perfusion 6 h after ICH for 72 hours.

2.2.2. ICH Model

The experimental ICH model was induced by injecting collagenase type IV (0.5 units in 2 μl saline) into the basal ganglia region using stereotaxic instruments. Mice were fixed on a stereotaxic apparatus under chloral hydrate anesthesia (10ml/kg, intraperitoneally); the skull was exposed to reveal bregma. A1-mm cranial bur hole was drilled in the skull (coordinates: 0.9 mm posterior to the bregma, 1.5 mm lateral to the midline), then, collagenase was infused into the right basal ganglia (4 mm deep from the dura mater) using a microinjector. The needle remained in place for an additional 15 min to prevent “back-leakage”. The Sham-operated mice were syringed with equivalent dosages of physiological saline. After surgery, the skull hole was sealed using bone wax and the incision was sutured. Animals were allowed to recover after successful ICH induction that was confirmed by Rosenberg’s neurological score [22].

2.2.3. Neurobehavior tests

As previously described[6,18-19], before sacrificing the animals for tissue collection, they were subjected to neurofunctional assessments using the modified Garcia tests. Notably, the modified Garcia scale involves an 18-point sensorimotor assessment that includes six individual tests. Each test has a score ranging

from 0 to 3, with a maximum score of 18. The individual tests evaluate spontaneous activity, response to side stroking, vibrissae touch, climbing, lateral turning, and forelimb walking.

2.2.4. Immunofluorescence detection

After intraperitoneal anesthesia, heart perfusion was performed using ice Phosphate-buffered saline (PBS) and 4% paraformaldehyde. The brain tissues of mice were removed on ice then placed in a 4% paraformaldehyde overnight at 4℃.Sucrose PBS buffer (20% and 30%) was used for dehydration at 4 °C until tissues were fully penetrated. After fixed embedding of OCT (optimal cutting temperature compound), frozen sections were coronally cut into 4-μm slices. The immunofluorescence methods were based on previously described methods.

2.2.5. Western blot

Total protein from brain tissue was collected, and their concentrations were determined using a BCA kit with a procedure similar to the foregoing cellular experiment methods.

2.3. Statistical analysis

All statistical and graphical analyses and were performed using SPSS 22.0 (IBM, Armonk, NY, USA) and GraphPad Prism 7.0 (https://www.graphpad.com/scientific-software/prism) software. All data were presented as the mean ± SEM (standard error of the mean). One-way analysis of variance (ANOVA) was performed for comparisons among multiple groups, whereas the SNK-q test was used for pairwise comparison between groups. A P-value of less than 0.05 $P < 0.05$ was considered statistically significant.

3 Results

3.1 Mortality, hemoglobin and neurological scores after ICH

All sham-operated mice survived. The total operative mortality rate of mice was estimated at 7.7% (n = 2) and was not significantly different among the surgical groups.

All ICH groups showed a significant decrease in modified Garcia scores and an increase in hemoglobin levels compared to that of the sham group at 72 hours after surgery ($p < 0.05$, Supplementary Fig A, B). In contrast with the ICH + vehicle, *Nrf2* agonist (Monascin and Xuezhikang) treatment significantly improved neurological deficits and reduced hemoglobin levels at 72 hours after ICH; conflicting results were found in *Nrf2*-/- group ($p < 0.05$, Supplementary Fig. A, B).

3.2 Nrf2 expression

Based on *in vitro* experiments, Western blot results showed that *Nrf2* was greatly improved in the monascin and Xuezhikang groups, while *Nrf2* was downregulated in the siRNA group compared to that in the normal control group (Fig. 1A-C). Furthermore, monascin and Xuezhikang promoted *Nrf2* expression *in vivo*, while they were significantly downregulated in the*Nrf2*-/- ICH group compared to that in the vehicle ICH group. Consistently, immunofluorescence detection confirmed similar patterns of *Nrf2* expression(Fig. 1D-F).

3.3 Trem1 and Trem2 protein expression

In the siRNA group, Western blot analysis revealed that the protein levels of *Trem2* expression were slightly downregulated, while that of *Trem1* expression was upregulated. However, monascin and xuezhikang reversed the protein expression of *Trem1* and *Trem2* along with *Nrf2* upregulation. Immunofluorescence results are similar to that of Western blot (Fig. 2A-F).

In contrast with the sham group, *in vivo Trem1* expression in all the ICH groups was up-regulated to varying degrees. Among them, *Trem1*expression in the vehicle and *Nrf2*-/- group was remarkably upregulated. Compared to vehicle group, *Trem1*expression was improved in *Nrf2*-/- group, while that in the monascin and Xuezhikang groups was attenuated. In contrast, the opposite results were observed for *Trem2*. The immunofluorescence results are roughly consistent with that of Western blot (Fig. 2G-L).

3.4.1. Phagocytosis of fluorescent bioparticles

In the phagocytic test of fluorescent bioparticles, the phagocytosis rate of the normal control group was approximately 2–3/cell, that of the siRNA group was about 1–2/cell, whereas that of monascin and Xuezhikang groups (about 4–5/cell) was significantly higher than that of the siRNA group (Fig. 3A).

3.4.2. Phagocytosis of erythrocytes

In the phagocytic test of erythrocytes, the phagocytosis rate of the normal control group was an approximately 1–2/microglial cell, that of the siRNA group was about 0–1/cell, whereas that of the monascin and Xuezhikang groups (about 3–6/cell) was significantly higher than that of the siRNA group (Fig. 3B).

3.5. Expression of CD80/CD206

In contrast with the normal group, cellular immunofluorescence demonstrated that both *CD80* and *CD206* in monascin and Xuezhikang groups were improved when *Nrf2* was upregulated; *CD206* expression was remarkably upregulated compared to that of *CD80*. However, *CD80* expression in the siRNA group was slightly upregulated, while that of *CD206* was downregulated. In this cellular WB, *CD206* expression in monascin and Xuezhikang groups was upregulated compared to that in the siRNA group, while that of *CD80* was reversed (Fig. 4A-D).

For *in vivo* experiment, Western blot results revealed that *CD80* expression in the four ICH groups was up-regulated compared to that in the sham group. Among them, a significant upregulation of *CD80* was

observed in the vehicle or *Nrf2*-/- group, and no significant difference was noted between the two groups. *CD206* expression in the monascin and Xuezhikang groups were significantly up-regulated, whereas *CD80* was down-regulated compared with the vehicle group. Immunofluorescence detection results are roughly consistent with that of WB (Fig. 4E-I).

3.6. Transformation of microglial neuroinflammation

Flow cytometry revealed that the total *CD80* expression in the siRNA group was upregulated, the *CD206*/ *CD80* ratio was downregulated, while the phenotype was transformed to the pro-inflammatory phenotype. In the monascin and Xuezhikang groups, the total *CD206* expression and *CD206*/ *CD80* ratio were upregulated, and the microglia were polarized toward the anti-inflammatory phenotype (Fig. 5).

3.7. TNF-α and BDNF protein expression

Nrf2-siRNA promoted the *TNF*-α protein expression, whereas monascin and Xuezhikang reversed the *TNF-a* inflammatory factor production instead of *BDNF*, particularly in the Xuezhikang group (Fig. 6A-D).

Unlike in the sham or vehicle group, the protein expression of *TNF-a* in the *Nrf2*-/- group was upregulated, while monascin and Xuezhikang reversed the *TNF-a* inflammatory factor production instead of *BDNF* ($p < 0.05$) (Fig. 6E-H).

4 Discussion

The present study has made the following observations: (1) The monascin and Xuezhikang groups promote *Nrf2* up-regulation in BV-2 microglia cells or C57BL/6 mice; while *Nrf2* was down-regulated in the siRNA-*Nrf2* group or *Nrf2*-/-group; (2) The monascin and Xuezhikang groups demonstrated a strong capacity to swallow fluorescent bioparticles or erythrocytes, and *Trem2*,*CD206*,*BDNF* expressions were upregulated; (3) On the other hand, *Nrf2* inhibition showed conflicting results, i.e., the *Trem2*,*CD206*,*BDNF* expressions were downregulated and the ability to swallow fluorescent bioparticles or erythrocytes was weak. (4) the expression of *Trem1*, *TNF-a* was upregulated in the *Nrf2*-/- group, while these expressions were reversed to varying degrees in the monasin and Xuezhikang groups compared with the vehicle group.

Microglia are the resident macrophages of the central nervous system (CNS) and undergo profound morphological and functional changes when activated. Traditionally, activated microglia initiates an immune response, release inflammatory mediators, and are vital regulators of the neuroinflammatory cascade[23, 24]. Alternatively, the activated microglia exerts their anti-inflammatory factors and phagocytic effect via changing their various surface receptors[25]; notably, the local extracellular and intracellular signals determine the features of microglia [26]. Pathogen-associated molecular patterns (PAMPs) or danger-associated molecular patterns (DAMPs) activate microglia to a pro-inflammation state[27]. In neuroinflammatory conditions including ICH and neurodegenerative diseases where pathogenic amyloid-β or hematoma residues accumulate, activation of microglia is promoted primarily via myeloid differentiation factor 88/TIR-domain-containing adaptor inducing interferon-β(MyD88/TRIF).The up-

regulation of nuclear factor kappa lightchain enhancer of activated B cells (NF-κB), varying amounts of inflammatory mediators are released, and neuroinflammatory are aggravated, affecting the survival of neuronal cells in the CNS[28, 29]. Primary mediators including *TNF*, *IL-1β*, and *IFNγ* are released, promoting the production of secondary mediators, including matrix metalloproteases (MMP), nitric oxide (NO), and arachidonic acid [30, 31]. Besides, *TNF-α* promotes the production of high-mobility group protein box-1 (*HMGB1*: a ligand of neuroinflammatory amplifier), which, in turn, stimulates microglia to release large amounts of *TNF-α* that activate additional microglia [12, 32, 33]. A self-feedback cascade loop has been reported in the process of microglial activation; these inflammatory signals are amplified by the self-feedback loop of microglial activation constructing an immune cascade inflammation network [23].

Nrf2 is a pleiotropic transcription factor extensively present in microglia. It is a steady-state regulator of cellular oxidative stress with a strong antioxidant capacity. The antioxidants produced, including heme oxygenase (*HO-1*), superoxide dismutase, catalase, glutathione sulfhydryl transferase, and haptoglobin (Hp)are activated [34]. Moreover, *Nrf2* is a vital target that regulates microglia in stroke and neurodegenerative diseases discovered in recent years. *Nrf2* upregulation downregulates *NF-κB* and promotes microglial transformation to the anti-inflammatory phenotype [35, 36].

Monascin is a novel type of *Nrf2* agonist[37], and an agonist of peroxidase of PPAR-, which suppresses oxidative stress in pathological conditions, promotes the absorption of hematoma and reduces intracerebral edema in our animal models of ICH[18, 19]. Xuezhikang is an extract of cholestin with monascin as its primary component; it is primarily used as traditional Chinese medicine (TCM) to fight atherosclerosis and exert anti-inflammatory effects by inhibiting toll-like receptor 4(*TLR4*)/ *NF-κB*[38,39].

Our research found that monascin/Xuezhikang promotes *Nrf2* upregulation of *Iba1*-marked microglia, and *Trem2* expression was significantly upregulated correspondingly; besides, their capacity to phagocytize erythrocytes or fluorescent bioparticles was improved after administering*Nrf2* agonist. In contrast, *Trem2* expression in *Nrf2*-knocked-down microglia or *Nrf2*-knocked-out mice was significantly downregulated, and their phagocytic capacity was significantly reduced.

Additionally, monascin/Xuezhikang effectively resists the neuroinflammation cascade of *Trem1* by up-regulating *Nrf2*. In all the ICH groups, *Trem1* was significantly up-regulated, indicating that *Trem1* is highly related to the neuroinflammation of ICH. *Trem1* expression in the *Nrf2*-/- group was significant, while the *Nrf2* agonists monascin and Xuezhikang reversed the *Trem1* expression. This implies that the change of *Nrf2* directly affects the expression of *Trem1*. The microglial cellular experiment further confirmed that Monascin/Xuezhikang effectively suppresses *Trem1* expression by upregulating *Nrf2*. However, *Trem2* demonstrated the opposite effects. The mechanism for this phenomenon remains vague, therefore, additional studies on *Trem1* and *Trem2* are necessary.

Here, monascin and Xuezhikang promoted the expression of the anti-inflammatory phenotype marker *CD206*, and the proportion of *CD206/80* was significantly increased. However, the expression of the pro-inflammatory phenotype marker *CD80* was upregulated, while that of *CD206* was downregulated after

Nrf2 was knocked down in microglia or knocked out in mice. These events indicate that the microglia were transformed into the anti-inflammatory phenotype after administration of monascin/Xuezhikang. Intriguingly, we found that *CD80* also was upregulated in the monascin and Xuezhikang groups in the cellular experiment, however, the upregulation in *CD206* was significantly greater than that of *CD80*, and the ratio of *CD206/CD80* was higher. This suggests that monascin and Xuezhikang may strengthen the immunity of microglia and are valuable for the survival of neurons. Nonetheless, additional studies are essential to improve its understanding. With the transformation of microglial neuroinflammation in the anti-inflammatory phenotype, the pro-inflammatory factor *TNF-α* was significantly decreased instead of the nerve repair factor *BDNF*, thus significantly inhibiting neuroinflammation. This is consistent with the findings reported in previous studies[40].

5 Conclusion

In conclusion, our findings showed that administration of *Nrf2* agonist monascin/Xuezhikang improves the phagocytic capacity of microglia, and improves anti-inflammation by promoting *Trem2*, *BDNF*, and *CD206* expressions, while inhibiting the pro-inflammatory cascade of *Trem1*, *TNF-α*, and *CD80* in microglia. Besides, *Nrf2* inhibition reversed the effects of *Nrf2* agonists. As such, *Nrf2* activation modulates hematoma clearance and neuroprotection after ICH, thereby providing a novel microglia-based approach for the treatment of ICH.

Abbreviations

BDNF: Brain-derived neurotrophic factor

CNS: Central nervous system

DAMPs: Danger-associated molecular patterns

HMGB1: High-mobility group protein box-1

HO-1: Heme oxygenase-1

Hp: Haptoglobin

ICH: Intracerebral hemorrhage

IFNγ: Interferon-gamma

IL-1β: Interleukin 1β

MMP: Matrix metalloproteases

Myd88: Myeloid differentiation factor 88

NF-κB: Nuclear factor-kappa lightchain enhancer of activated B cells

NO: Nitric oxide

Nrf2: Nuclear factor erythroid 2-related factor 2

PAMPs: Pathogen-associated molecular patterns

PPAR-: Peroxidase proliferator-activated receptor gamma

TCM: Traditional Chinese medicine

TLR4: Toll-like receptor 4

TNFα: Tumor necrosis factor-α

Trem1: Triggering receptors I expressed on myeloid cells

Trem2: Triggering receptors II expressed on myeloid cells

TRIF: TIR-domain-containing adaptor inducing interferon-β

Declarations

Ethics, consent, and permissions

All animal experiments were approved and conducted in accordance with the guidelines of the Ethics Committee of Shanxi Medical University, Shanxi, China. All surgical procedures were performed under anesthesia, and every effort was expended to minimize suffering.

Consent for publication

All authors have read the manuscript and have agreed to submit it in its current form for consideration for publication in the Journal of Neuroinflammation.

Availability of data and materials

All data and materials are available on request.

Competing interests

The authors declare that the research was conducted in the absence of any commercial or financial relationships that could be construed as a potential conflict of interest.

Funding

Project supported by Hainan Province Clinical Medical Center, National Natural Science Foundation of China (No.81771294; 82160237), and Shenzhen Municipal Science, Technology and Innovation Commission (No.JCYJ20190808161013492).

Author contributions

All authors listed have made a substantial, direct, and intellectual contribution to the work, and approved it for publication.

Acknowledgments

The authors thank all clinical personnel, epidemiologists, and county public health institutes personnel for their contribution to 2019-COVID outbreak control.

Consent to participate

Not applicable

References

1. Hemphill JC, III, Greenberg SM, Anderson CS, Becker K, Bendok BR, Cushman M, Fung GL, Goldstein JN, Macdonald RL, Mitchell PH, Scott PA, Selim MH, Woo D, Amer Heart Assoc Stroke C, Council Cardiovasc Stroke N, Council Clinical C (2015) Guidelines for the Management of Spontaneous Intracerebral Hemorrhage A Guideline for Healthcare Professionals From the American Heart Association/American Stroke Association. Stroke 46 (7):2032-2060. doi:10.1161/str.0000000000000069
2. van Asch CJJ, Luitse MJA, Rinkel GE, van der Tweel I, Algra A, Klijn CJM (2010) Incidence, case fatality, and functional outcome of intracerebral haemorrhage overtime, according to age, sex, and ethnic origin: a systematic review and meta-analysis. Lancet Neurology 9 (2):167-176. doi:10.1016/s1474-4422(09)70340-0
3. Gonzales NR (2013) Ongoing Clinical Trials in Intracerebral Hemorrhage. Stroke 44 (6):S70-S73. doi:10.1161/strokeaha.111.000563
4. Wang G, Wang L, Sun X-g, Tang J (2018) Haematoma scavenging in intracerebral haemorrhage: from mechanisms to the clinic. Journal of Cellular and Molecular Medicine 22 (2):768-777. doi:10.1111/jcmm.13441
5. Fang H, Chen J, Lin S, Wang P, Wang Y, Xiong X, Yang Q (2014) CD36-Mediated Hematoma Absorption following Intracerebral Hemorrhage: Negative Regulation by TLR4 Signaling. Journal of Immunology 192 (12):5984-5992. doi:10.4049/jimmunol.1400054
6. Wang G, Guo Z, Tong L, Xue F, Krafft PR, Budbazar E, Zhang JH, Tang J (2018) TLR7 (Toll-Like Receptor 7) Facilitates Heme Scavenging Through the BTK (Bruton Tyrosine Kinase)-CRT

(Calreticulin)-LRP1 (Low-Density Lipoprotein Receptor-Related Protein-1)-Hx (Hemopexin) Pathway in Murine Intracerebral Hemorrhage. Stroke 49 (12):3020-3029. doi:10.1161/strokeaha.118.022155

7. Nimmerjahn A, Kirchhoff F, Helmchen F (2005) Resting microglial cells are highly dynamic surveillants of brain parenchyma in vivo. Science (New York, NY) 308 (5726):1314-1318. doi:10.1126/science.1110647
8. Lan X, Han X, Li Q, Yang QW, Wang J (2017) Modulators of microglial activation and polarization after intracerebral haemorrhage. Nature reviews Neurology 13 (7):420-433. doi:10.1038/nrneurol.2017.69
9. Lan X, Han X, Li Q, Yang Q-W, Wang J (2017) Modulators of microglial activation and polarization after intracerebral haemorrhage. Nature Reviews Neurology 13 (7):420-433. doi:10.1038/nrneurol.2017.69
10. Tschoe C, Bushnell CD, Duncan PW, Alexander-Miller MA, Wolfe SQ (2020) Neuroinflammation after Intracerebral Hemorrhage and Potential Therapeutic Targets. Journal of Stroke 22 (1):29-46. doi:10.5853/jos.2019.02236
11. Zhang Z, Zhang Z, Lu H, Yang QW, Wu H, Wang J (2017) Microglial Polarization and Inflammatory Mediators After Intracerebral Hemorrhage. Molecular Neurobiology 54 (3):1874-1886. doi:10.1007/s12035-016-9785-6
12. Pelham CJ, Agrawal DK (2014) Emerging roles for triggering receptor expressed on myeloid cells receptor family signaling in inflammatory diseases. Expert Review of Clinical Immunology 10 (2):243-256. doi:10.1586/1744666x.2014.866519
13. Hall SC, Agrawal DK (2016) Toll-like receptors, triggering receptor expressed on myeloid cells family members and receptor for advanced glycation end-products in allergic airway inflammation. Expert Review of Respiratory Medicine 10 (2):171-184. doi:10.1586/17476348.2016.1133303
14. Zhou Y, Ulland TK, Colonna M (2018) TREM2-Dependent Effects on Microglia in Alzheimer's Disease. Frontiers in Aging Neuroscience 10. doi:10.3389/fnagi.2018.00202
15. Colonna M (2003) TREMs in the immune system and beyond. Nature reviews Immunology 3 (6):445-453. doi:10.1038/nri1106
16. Flores JJ, Klebe D, Rolland WB, Lekic T, Krafft PR, Zhang JH (2016) PPAR gamma-induced upregulation of CD36 enhances hematoma resolution and attenuates long-term neurological deficits after germinal matrix hemorrhage in neonatal rats. Neurobiology of Disease 87:124-133. doi:10.1016/j.nbd.2015.12.015
17. Zhao X-R, Gonzales N, Aronowski J (2015) Pleiotropic Role of PPAR gamma in Intracerebral Hemorrhage: An Intricate System Involving Nrf2, RXR, and NF-kappa B. Cns Neuroscience & Therapeutics 21 (4):357-366. doi:10.1111/cns.12350
18. Wang J, Wang G, Yi J, Xu Y, Duan S, Li T, Sun X-g, Dong L (2017) The effect of monascin on hematoma clearance and edema after intracerebral hemorrhage in rats. Brain Research Bulletin 134:24-29. doi:10.1016/j.brainresbull.2017.06.018

19. Fu P, Liu J, Bai Q, Sun X, Yao Z, Liu L, Wu C, Wang G (2020) Long-term outcomes of monascin - a novel dual peroxisome proliferator-activated receptor gamma/nuclear factor-erythroid 2 related factor-2 agonist in experimental intracerebral hemorrhage. Therapeutic Advances in Neurological Disorders 13. doi:10.1177/1756286420921083
20. Sun XG, Duan H, Jing G, Wang G, Hou Y, Zhang M (2019) Inhibition of TREM-1 attenuates early brain injury after subarachnoid hemorrhage via downregulation of p38MAPK/MMP-9 and preservation of ZO-1. Neuroscience 406:369-375. doi:10.1016/j.neuroscience.2019.03.032
21. Jia K-K, Ding H, Yu H-W, Dong T-J, Pan Y, Kong L-D (2018) Huanglian-Wendan Decoction Inhibits NF-kappa B/NLRP3 Inflammasome Activation in Liver and Brain of Rats Exposed to Chronic Unpredictable Mild Stress. Mediators of Inflammation 2018. doi:10.1155/2018/3093516
22. Rosenberg GA, Mun-Bryce S, Wesley M, Kornfeld M (1990) Collagenase-induced intracerebral hemorrhage in rats. Stroke 21 (5):801-807. doi:10.1161/01.Str.21.5.801
23. Liu L-r, Liu J-c, Bao J-s, Bai Q-q, Wang G-q (2020) Interaction of Microglia and Astrocytes in the Neurovascular Unit. Frontiers in Immunology 11. doi:10.3389/fimmu.2020.01024
24. Kierdorf K, Prinz M (2013) Factors regulating microglia activation. Frontiers in Cellular Neuroscience 7. doi:10.3389/fncel.2013.00044
25. Hu X, Leak RK, Shi Y, Suenaga J, Gao Y, Zheng P, Chen J (2015) Microglial and macrophage polarization -new prospects for brain repair. Nature Reviews Neurology 11 (1):56-64. doi:10.1038/nrneurol.2014.207
26. Jha MK, Lee W-H, Suk K (2016) Functional polarization of neuroglia: Implications in neuroinflammation and neurological disorders. Biochemical Pharmacology 103:1-16. doi:10.1016/j.bcp.2015.11.003
27. Rai V, Agrawal DK (2017) The role of damage- and pathogen-associated molecular patterns in inflammation-mediated vulnerability of atherosclerotic plaques. Canadian Journal of Physiology and Pharmacology 95 (10):1245-1253. doi:10.1139/cjpp-2016-0664
28. Sansing LH, Harris TH, Welsh FA, Kasner SE, Hunter CA, Kariko K (2011) Toll-like Receptor 4 Contributes to Poor Outcome after Intracerebral Hemorrhage. Annals of Neurology 70 (4):646-656. doi:10.1002/ana.22528
29. Zhou Y, Wang Y, Wang J, Stetler RA, Yang Q-W (2014) Inflammation in intracerebral hemorrhage: From mechanisms to clinical translation. Progress in Neurobiology 115:25-44. doi:10.1016/j.pneurobio.2013.11.003
30. Magaki SD, Williams CK, Vinters HV (2018) Glial function (and dysfunction) in the normal & ischemic brain. Neuropharmacology 134:218-225. doi:10.1016/j.neuropharm.2017.11.009
31. von Bernhardi R, Heredia F, Salgado N, Munoz P (2016) Microglia Function in the Normal Brain. In: VonBernhardi R (ed) Glial Cells in Health and Disease of the Cns, vol 949. Advances in Experimental Medicine and Biology. pp 67-92. doi:10.1007/978-3-319-40764-7_4
32. Ohnishi M, Katsuki H, Fukutomi C, Takahashi M, Motomura M, Fukunaga M, Matsuoka Y, Isohama Y, Izumi Y, Kume T, Inoue A, Akaike A (2011) HMGB1 inhibitor glycyrrhizin attenuates intracerebral

hemorrhage-induced injury in rats. Neuropharmacology 61 (5-6):975-980. doi:10.1016/j.neuropharm.2011.06.026

33. El Mezayen R, El Gazzar M, Seeds MC, McCall CE, Dreskin SC, Nicolls MR (2007) Endogenous signals released from necrotic cells augment inflammatory responses to bacterial endotoxin. Immunology letters 111 (1):36-44. doi:10.1016/j.imlet.2007.04.011
34. Cuadrado A, Rojo AI, Wells G, Hayes JD, Cousins SP, Rumsey WL, Attucks OC, Franklin S, Levonen A-L, Kensler TW, Dinkova-Kostova AT (2019) Therapeutic targeting of the NRF2 and KEAP 1 partnership in chronic diseases. Nature Reviews Drug Discovery 18 (4):295-317. doi:10.1038/s41573-018-0008-x
35. Wang Y, Huang Y, Xu Y, Ruan W, Wang H, Zhang Y, Saavedra JM, Zhang L, Huang Z, Pang T (2020) A Dual AMPK/Nrf2 Activator Reduces Brain Inflammation After Stroke by Enhancing Microglia M2 Polarization (vol 28, pg 141, 2018). Antioxidants & Redox Signaling 32 (3):213-214. doi:10.1089/ars.2017.7003.correx
36. Ren P, Chen J, Li B, Zhang M, Yang B, Guo X, Chen Z, Cheng H, Wang P, Wang S, Wang N, Zhang G, Wu X, Ma D, Guan D, Zhao R (2020) Nrf2 Ablation Promotes Alzheimer's Disease-Like Pathology in APP/PS1 Transgenic Mice: The Role of Neuroinflammation and Oxidative Stress. Oxidative Medicine and Cellular Longevity 2020. doi:10.1155/2020/3050971
37. Hsu W-H, Lee B-H, Pan T-M (2014) Monascin Attenuates Oxidative Stress-Mediated Lung Inflammation via Peroxisome Proliferator-Activated Receptor-Gamma (PPAR-gamma) and Nuclear Factor-Erythroid 2 Related Factor 2 (Nrf-2) Modulation. Journal of Agricultural and Food Chemistry 62 (23):5337-5344. doi:10.1021/jf501373a
38. Liang L, Shao W, Shu T, Zhang Y, Xu S, Guo L, Zhou Y, Huang H, Sun P (2019) Xuezhikang improves the outcomes of cardiopulmonary resuscitation in rats by suppressing the inflammation response through TLR4/NF-kappa B pathway. Biomedicine & Pharmacotherapy 114. doi:10.1016/j.biopha.2019.108817
39. Zheng J, Xiao T, Ye P, Miao D, Wu H (2017) Xuezhikang reduced arterial stiffness in patients with essential hypertension: a preliminary study. Brazilian Journal of Medical and Biological Research 50 (10). doi:10.1590/1414-431x20176363
40. Taylor RA, Sansing LH (2013) Microglial Responses after Ischemic Stroke and Intracerebral Hemorrhage. Clinical & Developmental Immunology. doi:10.1155/2013/746068

Figures

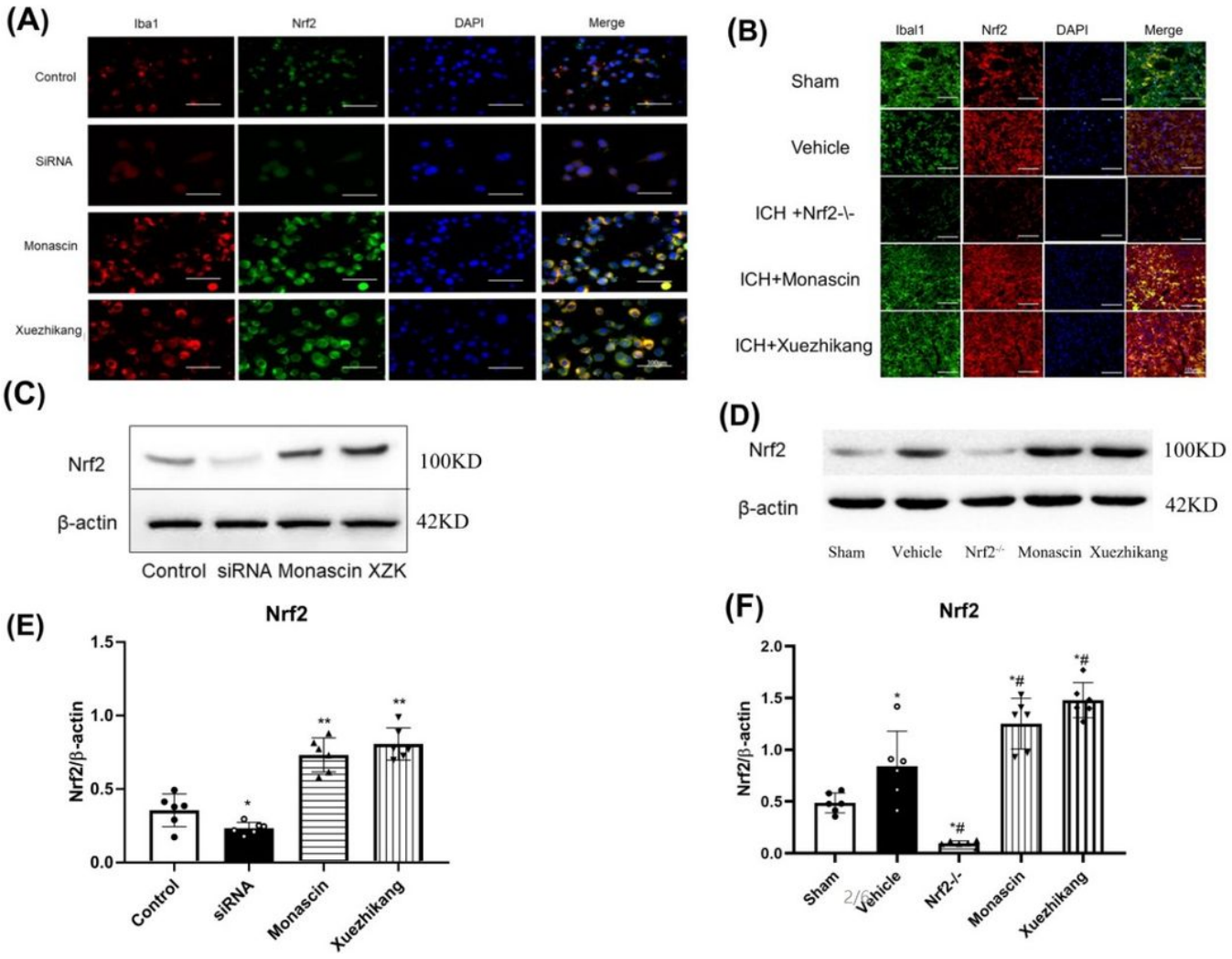

Figure 1

Immunofluorescence (*in vitro*×400 and *in vivo*×200) and Western blot protein expression of *Nrf2*.

Red fluorescence represents *Iba1* expression, green fluorescence indicates *Nrf2* expression, while blue fluorescence depicts nuclear DAPI staining. “Merge” represents the superposition of the first three images. Western blot analysis and immunofluorescence detection showed that *Nrf2* production of microglia was upregulated in the monascin/Xuezhikang groups, while was downregulated in the siRNA group compared to that in the normal group(A)-(C) (*, $p< 0.05$ vs. the control and **, $p< 0.01$ vs. the control, WB: Western blot; *Nrf2*: nuclear factor erythroid 2-related factor 2; *Iba1*: ionized calcium-binding protein 1, microglial marker). For*in vivo* experiment, red fluorescence depicts *Nrf2* expression, while green fluorescence represents *Iba1* expression. Monascin and Xuezhikang promoted *Nrf2*expression, while they were significantly downregulated in *Nrf2*-/- group compared to that in the sham or vehicle group. Representative images of immunofluorescence and Western blot assays are shown (D)-(F) (*, $p< 0.05$ vs. sham and #, $p< 0.05$ vs. ICH + vehicle were statistically significant)

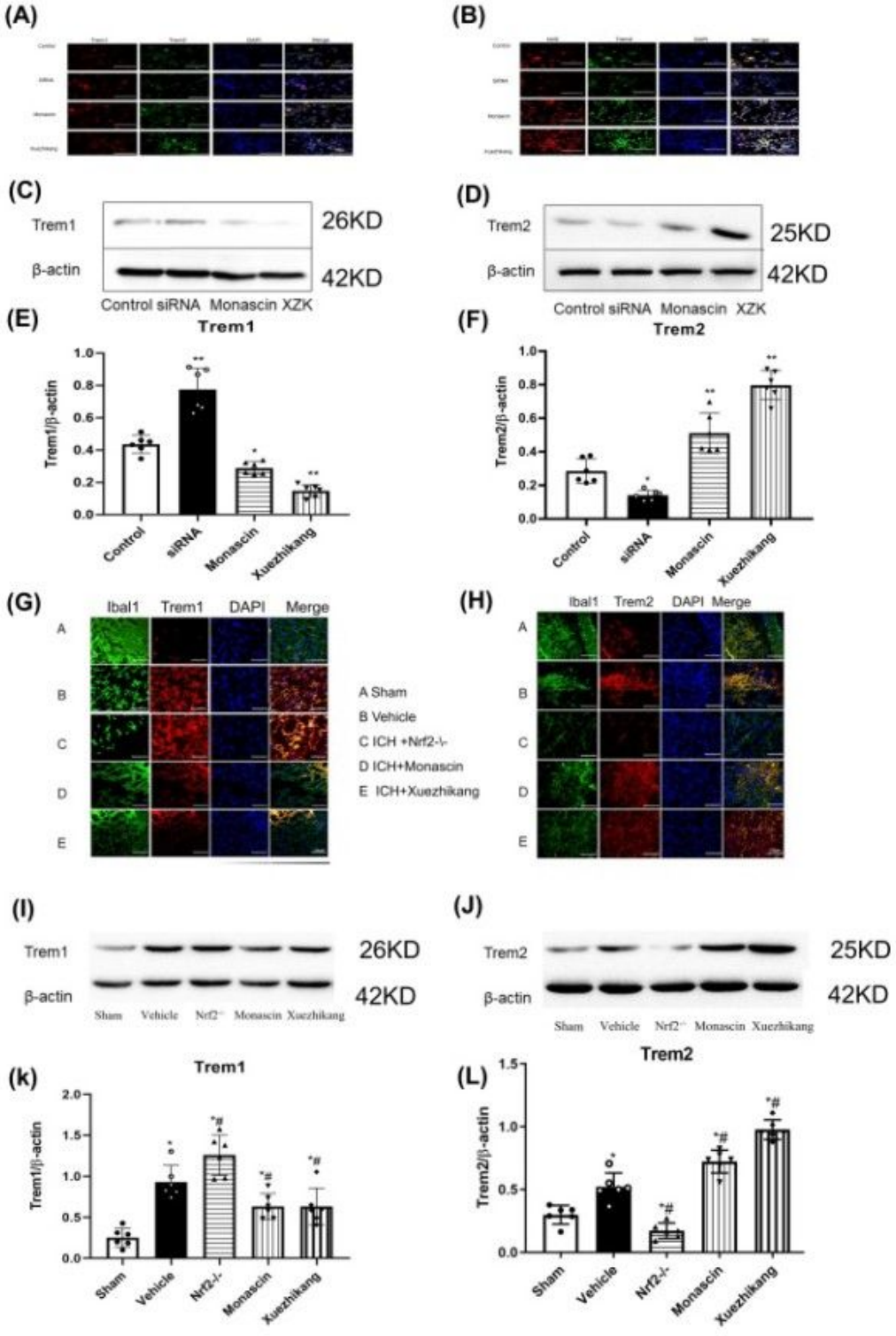

Figure 2

Protein expression of *Trem1*/ *Trem2* determined using immunofluorescence (*in vitro*×400 and *in vivo*×200) and Western blot.

Red fluorescence represents *Trem1* or *Nrf2* expression, green fluorescence depicts *Trem2* expression, while blue fluorescence is nuclear DAPI staining. “Merge” represents the superposition of the first three

images. In the siRNA group, immunofluorescence or Western blot results revealed that the protein levels of *Trem2* expression were slightly downregulated, while that of *Trem1*expression was upregulated. Nonetheless, monascin and Xuezhikang reversed the protein *Trem1* and *Trem2* expression along with *Nrf2*upregulation (A)-(F). Red fluorescence (*in vivo* experiment) represents *Trem1* and *Trem2* expression, while green fluorescence is *Nrf2* expression. Unlike in the sham group, *Trem1*expression in all the ICH groups was up-regulated to varying degrees. In contrast with the vehicle group, *Trem1*expression was improved in the *Nrf2*-/- group, whereas that in monascin and Xuezhikang groups was attenuated. However, *Trem2* showed upregulation in monascin and Xuezhikang groups(G)-(L) (*Trem1*: Triggering receptor I expressed on myeloid cells; *Trem2*: Triggering receptor II expressed on myeloid cells).

Fig 3A

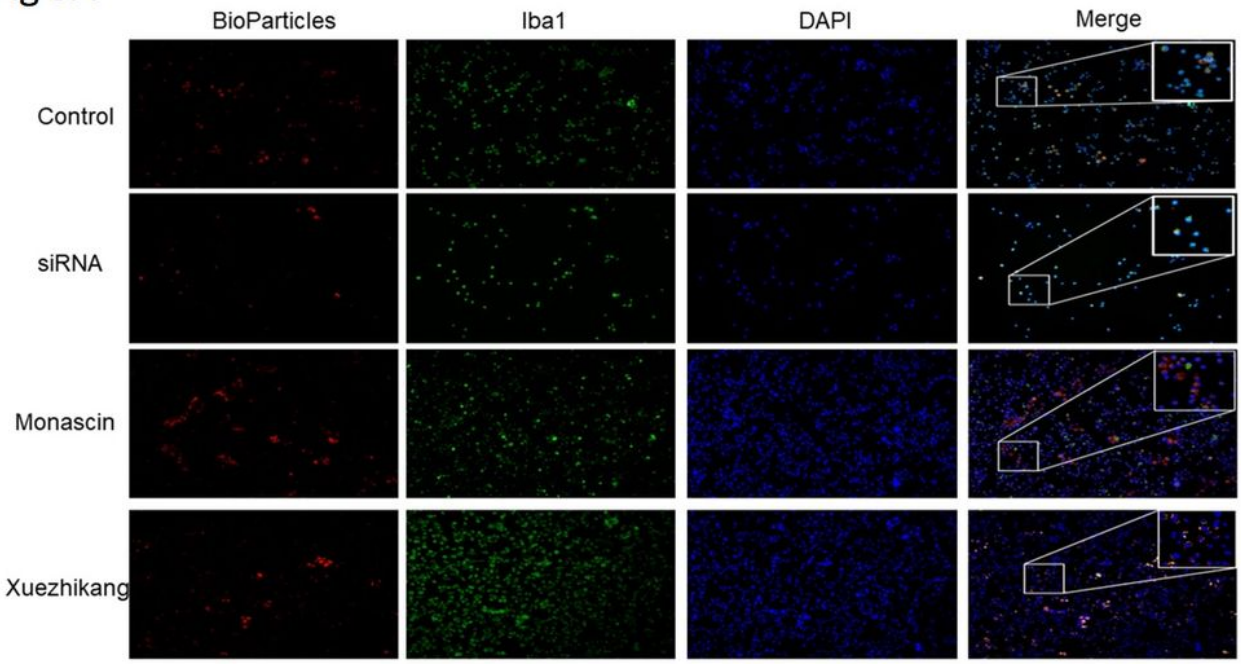

Fig 3B

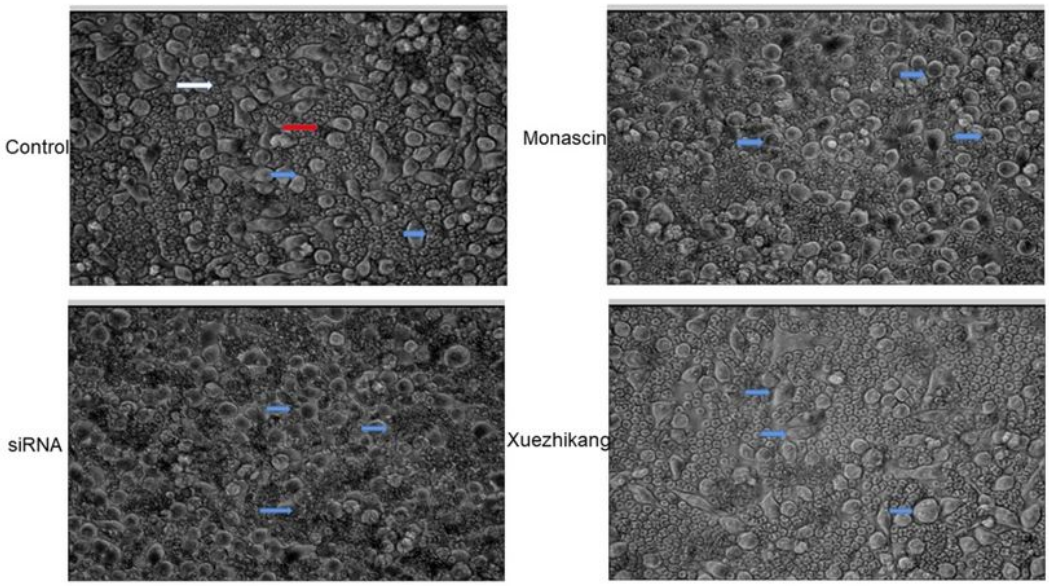

Figure 3

3A. Phagocytosis test of fluorescent bioparticles (immunofluorescence ×100)

Green fluorescence is the *Iba1* cells, red fluorescence is the fluorescent bioparticles, and blue fluorescence is the nuclear DAPI staining. “Merge” represents the superposition of the first three images. The average phagocytosis of the fluorescent bioparticles was about 2-3/cell in the normal control group, about 1-

2/cell in the siRNA group, and 4-5/cell in the monascin/Xuezhikang groups. The phagocytosis rates were significantly increased in the monascin and Xuezhikang groups.

3B. Phagocytosis test of erythrocytes (×400)

The white arrow is microglia, the red arrow is erythrocytes, while the blue arrow represents the microglia that swallowed erythrocytes. The average phagocytosis of the erythrocytes was an approximately 1-2/microglial cell in the normal control group, 0-1/cell in the siRNA group, and 3-6/cell in the monascin and Xuezhikang groups. The phagocytosis rates were significantly increased in the monascin and Xuezhikang groups.

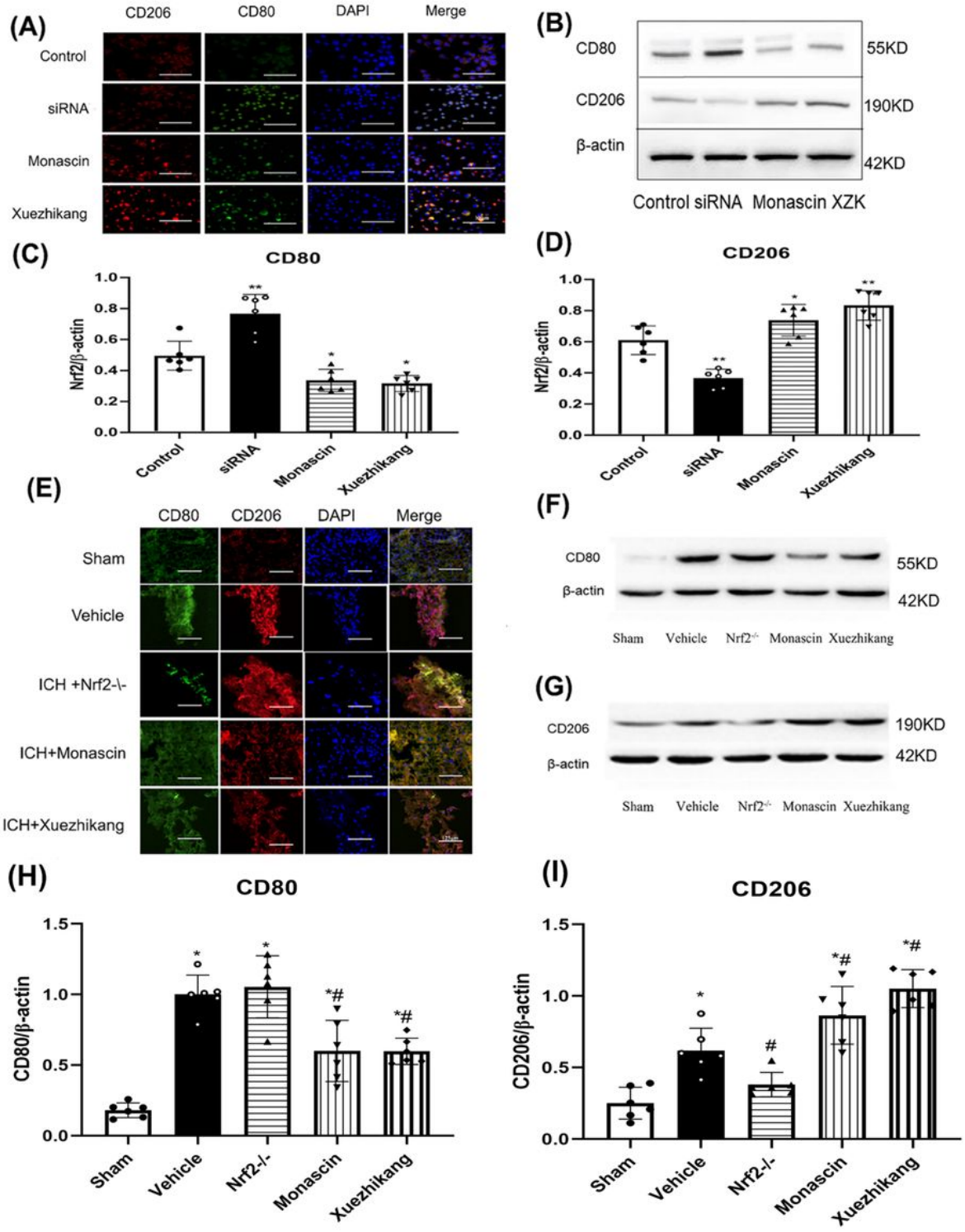

Figure 4

Expression of *CD80*/ *CD206* detected by immunofluorescence (*in vitro*×400 and *in vivo*×200) and Western blot.

The green fluorescence represents *CD80*, the red fluorescence is CD206, while the blue fluorescence is nuclear DAPI staining. “Merge” represents the superposition of the first three images. Unlike in the normal

group, cellular immunofluorescence showed that both *CD80* and *CD206* were improved when *Nrf2* was elevated in the monascin and Xuezhikang groups; *CD206* expression was significant compared to that of *CD80*. In this cellular WB, *CD206* expression in monascin and Xuezhikang groups was statistically elevated compared to that in the siRNA group, however, *CD80* expression was reversed (A)-(D). For *in vivo* experiment, the red fluorescence represents *CD80*, the green fluorescence is *CD206*. Unlike in the sham group, Western blot analysis revealed that *CD80* expression in the four groups of ICH was up-regulated; a significant *CD80* upregulation was observed in the vehicle or *Nrf2-/-* group. *CD206* expression in the monascin and Xuezhikang groups was significantly up-regulated, whereas that of CD80 was down-regulated compared with the vehicle group. The results of immunofluorescence detection are roughly consistent with that of WB (E)-(I).

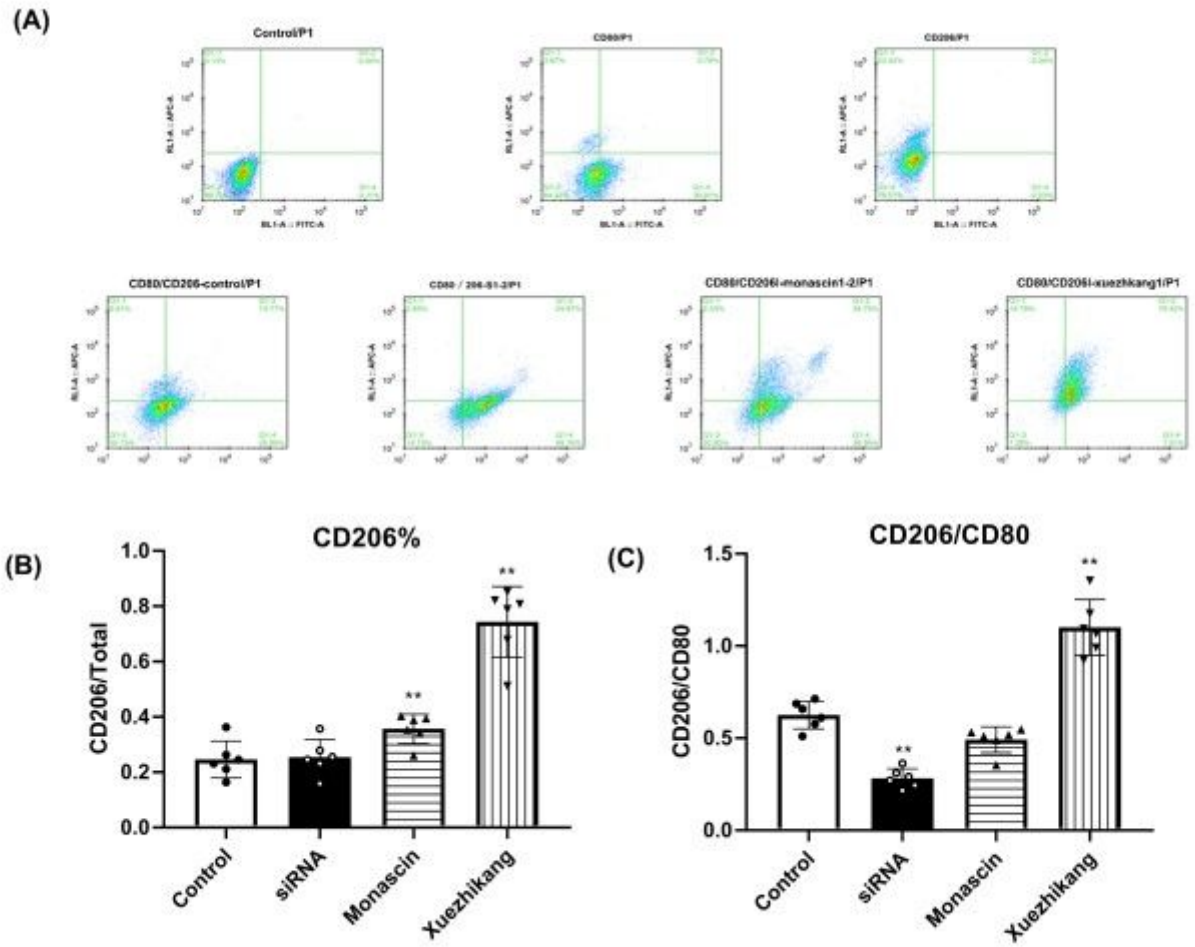

Figure 5

Transformation of microglial neuroinflammation as shown by flow cytometry

The ratio of *CD206/CD80* and the total expression of *CD206*was significantly upregulated in the monascin and Xuezhikang groups, and the microglial phenotype was transformed to the anti-inflammatory phenotype (green fluorescent FITC: *CD80*; red fluorescent APC: *CD206*).

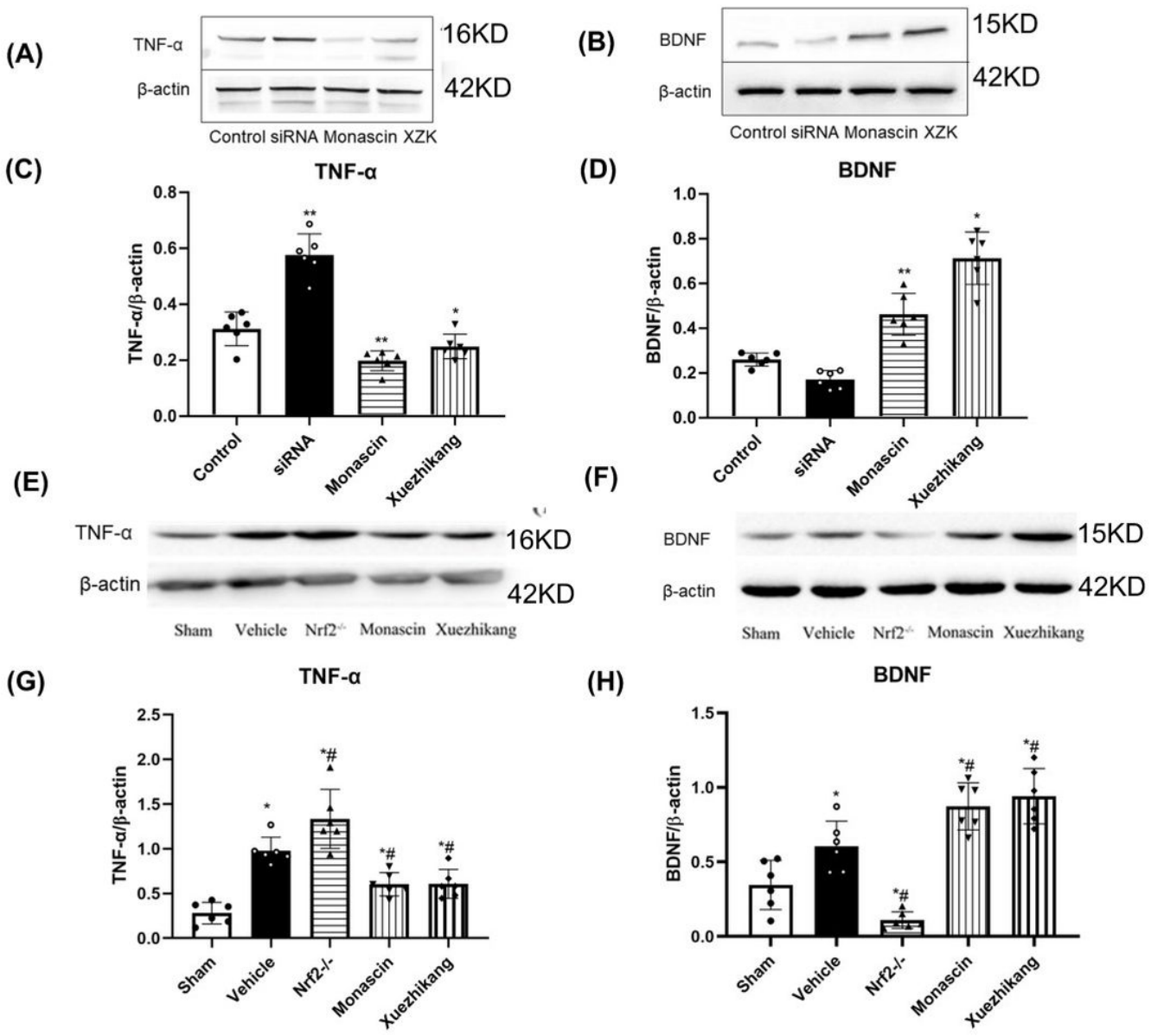

Figure 6

Protein expression of inflammatory factor *TNF-α* and *BDNF* by Western blot

The protein expression of *BDNF* was significantly upregulated in the monascin and Xuezhikang groups; however, it was downregulated in the *Nrf2*-siRNA group(A)-(D) or in the *Nrf2*-/- group(E)-(H) *TNF-α* protein expression downregulated in the monascin and Xuezhikang groups while it was upregulated in the *Nrf2*-siRNA or *Nrf2*-/- group (*TNF-α*: tumor necrosis factor α; *BDNF*: brain-derived growth factor)

Supplementary Files

This is a list of supplementary files associated with this preprint. Click to download.

- SupplementalFigA.tif

- SupplementalFigB.tif